

The impact of demographic factors on the accumulated number of COVID-19 cases per capita in Europe and the regions of Ukraine in the summer of 2021

Igor Nesteruk

Institute of Hydromechanics, National Academy of Sciences of Ukraine, Kyiv, Ukraine

Igor Sikorsky Kyiv Polytechnic Institute, Kyiv, Ukraine.

inesteruk@yahoo.com

Oleksii Rodionov

Private consulting office, Kyiv, Ukraine

ABSTRACT

The accumulated number of COVID-19 cases per capita is an important characteristic of the pandemic dynamics that may also indicate the effectiveness of quarantine, testing and vaccination. As this value increases monotonically over time, the end of June 2021 was chosen, when the growth rate in Ukraine and the vast majority of European countries was small. This allowed us to draw some intermediate conclusions about the influence of the volume of population, its density, and the level of urbanization on the accumulated number of laboratory-confirmed cases per capita in European countries and regions of Ukraine. A simple analysis showed that the number of cases per capita does not depend on these demographic factors, although it may differ by about 4 times for different regions of Ukraine and more than 9 times for different European countries. The number of COVID-19 per capita registered in Ukraine is comparable with the same characteristic in other European countries but much higher than in China, South Korea and Japan.

Keywords: COVID-19 pandemic, epidemic dynamics in Europe, epidemic dynamics in Ukraine, mathematical modeling of infection diseases, statistical methods.

Introduction

The accumulated number of COVID-19 cases per capita (CC) may indicate the effectiveness of quarantine, testing, vaccination, and also characterizes the virulence of coronavirus strains circulating in a particular region. The CC values increase monotonically over time, so it is important to fix the appropriate time and compare these values for different countries and regions. In particular, in this study we take the end of June 2021, when the CC growth rate in Ukraine and the vast majority of European

NOTE: This preprint reports new research that has not been certified by peer review and should not be used to guide clinical practice. countries was small. The CC numbers are regularly reported by World Health

Organization, [1] and COVID-19 Data Repository by the Center for Systems Science and Engineering (CSSE) at Johns Hopkins University (JHU), [2].

The impact of some eco-demographic factors on the COVID-19 pandemic dynamics was studied in [3-19]. The influence of the population volume N_{pop} on the final sizes V_{∞} of the first pandemic waves in different countries and regions was studied in [19] and compared with the real CC values at fixed moments of time. In particular, relative final size of the first epidemic wave \bar{V}_{∞} was approximated by following equations:

$$\bar{V}_{\infty} \equiv \frac{V_{\infty}}{N_{pop}} = 0.0018546 N_{pop}^{-0.11} \quad (1)$$

$$\bar{V}_{\infty} \equiv \frac{V_{\infty}}{N_{pop}} = 0.0013101 N_{pop}^{0.0778} \quad (2)$$

with the use results of SIR simulations for $n=13$ countries and regions and the results for $n=11$ (without mainland China and South Korea), respectively.

In this paper we will study the influence of the volume of population N_{pop} , its density, and the level of urbanization N_{ubr}/N_{pop} (N_{ubr} is the number of people living in cities) on the accumulated number of laboratory-confirmed cases per capita in European countries and regions of Ukraine.

Data

We will use the data set regarding the numbers of laboratory-confirmed COVID-19 cases in the regions of Ukraine accumulated at the time June 27, 2021 and registered by national statistics, [20]. The corresponding CC numbers (per 100 persons of population) and demographic data sets for Ukrainian regions [21] are shown in Table 1. As the information from the regions of Ukraine fully or partially occupied by the Russian Federation is inaccurate, we excluded from consideration Donetsk and Luhansk regions, Crimea and Sevastopol. It can be seen that CC values vary from 2.25 (Kirovohrad oblast) to 8.84 (Chernivtsi oblast). Rather high CC values were registered in Zhytomyr, Khmelnytskyi, Kyiv (oblast and city), and Sumy regions that are not in the west of Ukraine with traditionally close ties with the EU countries.

The CC figures (per 1,000,000 persons of population) accumulated at the time June 28, 2021 and registered by JHU, [2] are shown in Table 2, which contains also the demographic data sets for European countries taken from [22-24]. The highest CC levels were registered in Andorra - 18%, Montenegro – 16%, Czech Republic - 15.5%, San

Marino - 15%, Slovenia - 12.4%. The populations of these countries are not very high as well as populations of Iceland and Finland where the lowest CC values were registered (1.9% and 1.7%, respectively). More than a tenfold difference in values raises a reasonable question about its causes. They may be related to the population density or the level of urbanization. A possible relationship with these factors will be explored further.

Oblast (region)	Population, N_{pop} , [21]	Urban population, N_{ubr} , [21]	Population density (number of people per square kilometer), [21]	Accumulated number of laboratory- confirmed cases per hundred, [20]
Vinnitsia	1 545 416	799 385	58.29	4.67
Volyn	1 031 421	539 179	51.2	6.06
Dnipropetrovsk	3 176 648	2 668 744	99.54	4.33
Zhytomyr	1 208 212	716 457	40.5	7.43
Zakarpattia	1 253 791	465 904	98.13	4.98
Zaporizhzhia	1 687 401	1 306 231	62.08	6.30
Ivano-Frankivsk	1 368 097	606 764	98.23	6.38
Kyiv (oblast)	1 781 044	1 105 383	63.31	7.12
Kirovohrad	933 109	591 944	37.95	2.25
Lviv	2 512 084	1 534 040	115.06	5.52
Mykolaiv	1 119 862	768 022	45.53	6.34
Odesa	2 377 230	1 597 062	71.37	5.95
Poltava	1 386 978	867 201	48.25	5.70
Rivne	1 152 961	548 088	57.51	6.93
Sumy	1 068 247	741 430	44.82	7.43
Ternopil	1 038 695	473 727	75.14	6.82
Kharkiv	2 658 461	2 158 121	84.62	5.66
Kherson	1 027 913	631 317	36.12	3.53
Khmelnyskyi	1 254 702	720 752	60.82	7.18
Cherkasy	1 192 137	678 682	57.04	6.97
Chernivtsi	901 632	390 551	111.35	8.94
Chernihiv	991 294	649 063	31.11	5.92
Kyiv (city)	2 967 360	2 967 360	3536.78	7.22

Table 1. Demographic characteristics and the accumulated number of laboratory-confirmed COVID-19 cases in the regions of Ukraine as of June 27, 2021

Country	Population, [22]	Urbanization N_{ubr}/N_{pop} , %, [23]	Population density (per square km), [24]	Total cases per million, [2]
Monaco	38682	100	15,47	65615.126
Holy See (Vatican City)	801	100	2,273	33374.536
Malta	514564	95	1,447	69330.229
San Marino	33785	97	561	150008.84
Netherlands	17059560	91	416	99886.646
Belgium	11482178	98	384	93486.963
United Kingdom	67141684	83	270	70284.988
Liechtenstein	37910	14	245	79555.288
Luxembourg	604245	91	243	112850.972
Germany	83124418	77	225	44576.917
Italy	60627291	70	207	70432.141
Switzerland	8525611	74	204	81198.962
Andorra	77006	88	183	179667.379
Denmark	5752126	88	136	50743.387
Czech Republic	10665677	74	136	155658.773
Poland	37921592	60	122	76088.436
Portugal	10256193	65	112	85856.051
Slovakia	5453014	54	111	71720.074
Albania	2882740	60	107	46046.633
Austria	8891388	66	106	72206.875
France	64990511	80	105	86325.089
Hungary	9707499	71	105	83645.21
Turkey	82340088	75	105	64196.94
Slovenia	2077837	55	104	123742.383
Moldova	4051944	43	99	63613.375
Spain	46692858	80	99	81117.733
Serbia	8802754	56	91	105279.579
Romania	19506114	54	89	56174.491
North Macedonia	2082957	58	83	74722.806
Greece	10522246	79	80	40416.745
Bosnia and Herzegovina	3323925	48	75	62481.731
Croatia	4156405	57	75	87610.845
Ireland	4818690	63	74	55002.07
Ukraine	44246156	69	73	52556.15
Bulgaria	7051608	75	63	60682.066
Belarus	9452617	78	46	44001.045
Montenegro	627809	67	44	159544.758
Lithuania	2801264	68	42	102372.965
Latvia	1928459	68	29	72759.97
Estonia	1322920	69	27	98740.406
Sweden	9971638	87	23	107819.278
Norway	5337962	82	17	24116.983
Finland	5522576	85	16	17176.113
Iceland	336713	94	3	19208.791

Table 2. Demographic characteristics and the accumulated number of laboratory-confirmed COVID-19 cases in European countries as of June 28, 2021

Results

The CC values (per 100 persons, blue “crosses”) versus the volume of population, its density and the urbanization level are shown in Figs. 1-6. We have used datasets from Tables 1 and 2. The best fitting lines (black) were calculated by the least squares method [25]. The linear regression was used to calculate the regression coefficient r and the coefficients a and b of corresponding straight lines, [25]:

$$CC = a + bx \quad (3)$$

where x is the volume of population N_{pop} (Figs. 1 and 2), its density per square km (Figs. 3 and 4), and the urbanization level N_{urb}/N_{pop} (Figs. 5 and 6).

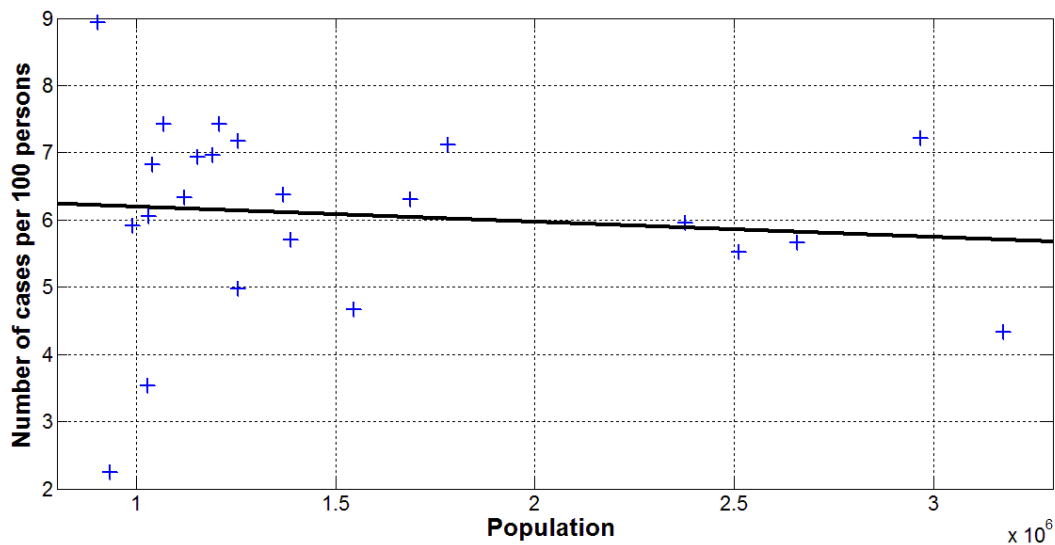


Fig.1. COVID-19 cases per 100 persons versus volume of population registered in the regions of Ukraine as of June 27, 2021

Blue “crosses” show the accumulated number of laboratory-confirmed cases per 100 persons (Table 1). The best fitting line (3) is shown in black.

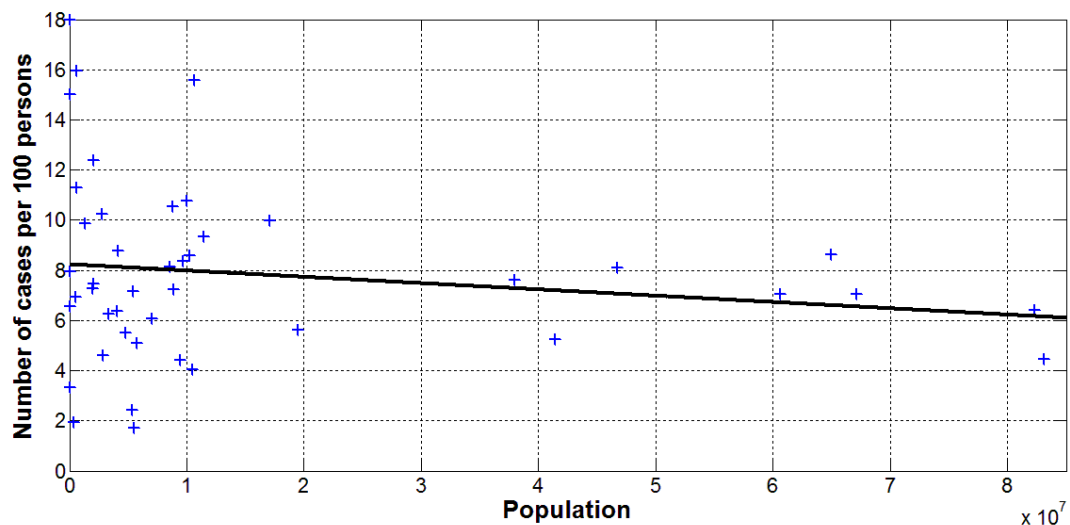


Fig.2. COVID-19 cases per 100 persons versus volume of population registered in the European countries as of June 28, 2021

Blue “crosses” show the accumulated number of laboratory-confirmed cases per 100 persons (Table 2). The best fitting line (3) is shown in black.

Figs. 1 and 2 illustrate that there is no visible correlation between CC values and the volume of population both in the case of Ukrainian regions and European countries. We can see only slight decreasing of CC values with increasing of N_{pop} . The same tendency was revealed in [19] for the \bar{V}_{∞} (see eq. (1)). Corresponding values of r , a , b and the number n of regions or countries taken for calculations are shown in Table 3.

Number of figure	n	Correlation coefficient r	Optimal values of parameters a in (3)	Optimal values of parameters b in (3)	Experimental value of the Fisher function F , eq. (4), $m=2$	Critical value of Fisher Function $F_c(I, n-2)$ for the confidence level 0.1, [26]
1	23	-0.1082	6.4203	-2.2551e-007	0.2486	2.96
2	44	-0.1607	8.2330	-2.5094e-008	1.1132	2.84
3	23	0.1792	5.9935	3.5699e-004	0.6967	2.96
4	44	-0.0953	8.0331	-7.7955e-004	0.3848	2.84
5	23	-0.1024	6.6956	-1.0123	0.2224	2.96
6	44	-0.0019	7.8739	-0.0394	1.5088e-004	2.84

Table 3. Optimal values of parameters in eq. (3), correlation coefficients and the results of Fisher test applications.

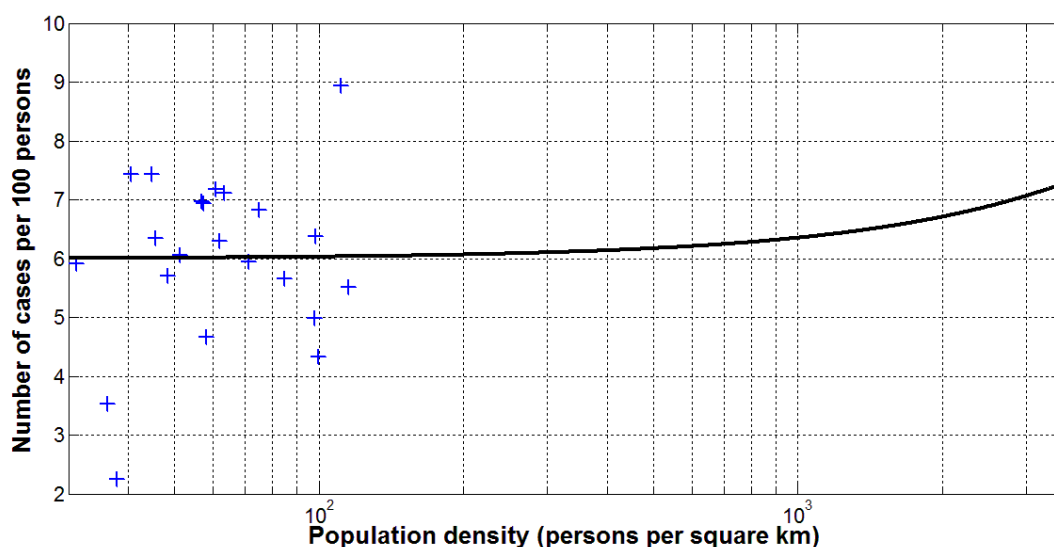


Fig. 3. COVID-19 cases per 100 persons versus density of population (per square km) registered in the regions of Ukraine as of June 27, 2021

Blue “crosses” show the accumulated number of laboratory-confirmed cases per 100 persons (Table 1). The best fitting line (3) is shown in black.

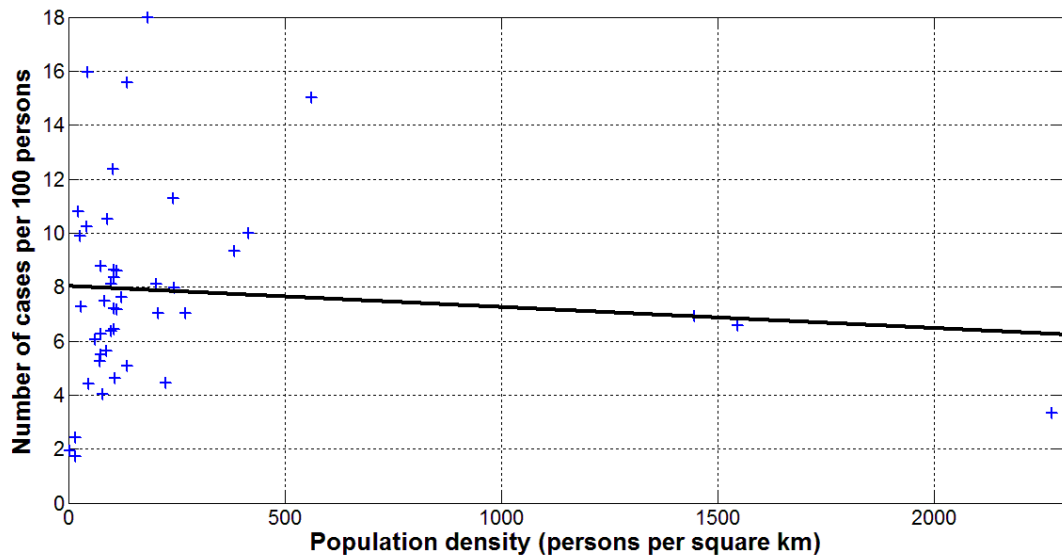


Fig. 4. COVID-19 cases per 100 persons versus density of population (per square km) registered in the European countries as of June 28, 2021

Blue “crosses” show the accumulated number of laboratory-confirmed cases per 100 persons (Table 2). The best fitting line (3) is shown in black.

Figs. 3-6 and Table 3 illustrate that CC values do not correlate with the density of population and the urbanization level both in the case of Ukrainian regions and European countries. In Fig. 3 we can see only slight increasing of CC values with increasing of the density of population in Ukrainian regions. Opposite trend is visible in Fig. 4 for European countries. The corresponding values of the correlation coefficient and parameter b have opposite signs. In Figs. 5 and 6 we can see a slight decreasing of CC values with increasing the level of urbanization N_{ubr}/N_{pop} .

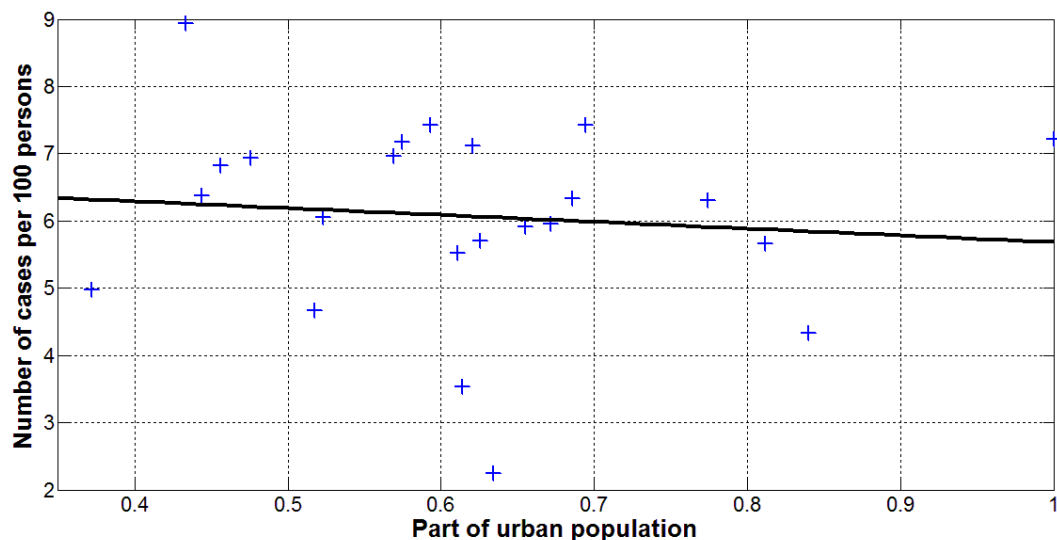


Fig. 5. COVID-19 cases per 100 persons versus part of the urban population N_{ubr}/N_{pop} registered in the regions of Ukraine as of June 27, 2021

Blue “crosses” show the accumulated number of laboratory-confirmed cases per 100 persons (Table 1). The best fitting line (3) is shown in black.

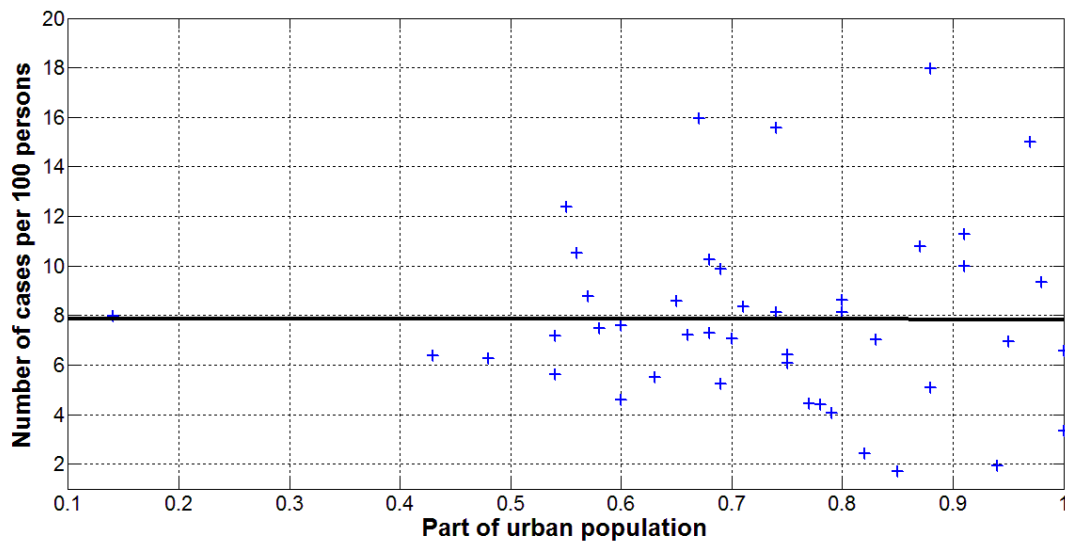


Fig. 6. COVID-19 cases per 100 persons versus part of the urban population N_{ubr}/N_{pop} population registered in the European countries as of June 28, 2021
Blue “crosses” show the accumulated number of laboratory-confirmed cases per 100 persons (Table 2). The best fitting line (3) is shown in black.

Discussion

We can use also the F-test for the null hypothesis that says that the proposed linear relationship (3) fits the data sets. The experimental values of the Fisher function can be calculated with the use of the formula:

$$F = \frac{r^2(n-m)}{(1-r^2)(m-1)} \quad (4)$$

where $m=2$ is the number of parameters in the regression equation, [25]. The corresponding experimental values F are shown in Table 3. They have to be compared with the critical values $F_C(k_1, k_2)$ of the Fisher function at a desired significance or confidence level ($k_1 = m-1$, $k_2 = n-m$, see, e.g., [26]). Comparisons of the values in the last two columns of Table 3 show that the critical values are much higher than the experimental F values. It means that the data sets presented in Tables 1 and 2 do not support the linear relationship (3).

We have checked also the non-linear dependences:

$$CC = \delta x^n \quad (5)$$

instead of (3) as it was done in [19, 27, 28]. Similar to the case of linear dependence (3), the calculations showed that corresponding values $|r| \ll 1$ and $F_c(k_1, k_2) > F$. It means that hypothesis (5) was not also supported by the datasets presented in Tables 1 and 2.

Very different CC values registered in the regions of Ukraine and European countries could be a result of different coronavirus strains, quarantine measures, testing, tracing and isolating patients. One more reason may be the large number of unregistered cases observed in many countries [29-33]. Estimates for Ukraine and Qatar made in [29, 33] showed that the real number of cases is about 4-5 times higher than registered and reflected in the official statistics. Similar estimates can be made for the regions of Ukraine and other European countries.

If we apply the visibility coefficients $\beta_{10}=3.7$ and $\beta_3=5.308$ calculated for the Ukraine and Qatar (see [29, 33]) and take accumulated numbers of laboratory-confirmed cases, the CC values could be estimated as 20% in Ukraine and 42% in Qatar (as of the end of June 2021). Such a high percentage of people who catch the coronavirus infection can significantly affect the evaluation of the vaccination efficiency. Probably this is why we do not yet see the effect of vaccination on the pandemic dynamics in Qatar, [34].

The highest CC values registered in Europe are close to ones in other regions, e.g., Seychelles-15.8%, Bahrain-15.6%. The lowest CC values in Europe is much higher than in Vanuatu, Micronesia, Tanzania (around 0.001%), and China (0.006%). Very small CC values in the WHO Western Pacific region (e.g. Vietnam – 0.017%; Laos - 0.029%; South Korea, Cambodia - 0.3%; and 0.63% for Japan) need special investigations, but let us express some hypotheses.

First of all the COVID-19 pandemic probably started in this region in August 2019, [18]. It means that first cases were not identified and registered during at least 4 months. Probably these first cases were not very severe and the symptoms were not so pronounced. Presumably mutations of the coronavirus made it more pathogenic and sick people became more noticeable in December 2019. But previous cases were not taken into account in the statistics. Recent DNA investigations of East Asia population reported the presence of coronavirus around 20,000 years ago [35]. Probably, the population of this region had a collective immunity to pathogens similar to Covid-19 before the pandemic.

References

1. World Health Organization. “Coronavirus disease (COVID-2019) situation reports”. <https://www.who.int/emergencies/diseases/novel-coronavirus-2019/situation-reports/>. Retrieved Oct. 3, 2020.
2. COVID-19 Data Repository by the Center for Systems Science and Engineering (CSSE) at Johns Hopkins University (JHU). <https://github.com/owid/covid-19-data/tree/master/public/data>
3. Byass, P. Eco-epidemiological assessment of the COVID-19 epidemic in China, January-February 2020. medRxiv 2020, doi:10.1101/2020.03.29.20046565.
4. Dehning J. et al. Inferring COVID-19 spreading rates and potential change points for case number forecasts. Preprint, ArXiv:2004.01105(2020).
5. Distante, C.; Gadelha Pereira, I.; Garcia Goncalves, L.M.; Piscitelli, P.; Miani, A. Forecasting Covid-19 Outbreak Progression in Italian Regions: A model based on neural network training from Chinese data. medRxiv 2020.
6. Hamzah, F.; Binti, A.; Lau, C.; Nazri, H.; Ligot, D.V.; Lee, G.; Tan, C.L. CoronaTracker: Worldwide COVID-19 Outbreak Data Analysis and Prediction. Bull. World Health Organ. 2020, 1, 32.
7. Fanelli, D.; Piazza, F. Analysis and forecast of COVID-19 spreading in China, Italy and France. Chaos Solitons Fractals 2020, 134, 109761.
8. Webb, G.F.; Magal, P.; Liu, Z.; Seydi, O. A model to predict COVID-19 epidemics with applications to South Korea, Italy, and Spain. medRxiv 2020.
9. Distante, C.; Piscitelli, P.; Miani, A. Covid-19 Outbreak Progression in Italian Regions: Approaching the Peak by the End of March in Northern Italy and First Week of April in Southern Italy. Int. J. Environ. Res. Public Health 2020, 17, 3025.
10. KY Ng, MM Gui. COVID-19: Development of a robust mathematical model and simulation package with consideration for ageing population and time delay for control action and resusceptibility. Physica D: Nonlinear Phenomena, Volume 411, October 2020, 132599
<https://doi.org/10.1016/j.physd.2020.132599>
11. Diego Carvalho, Rafael Barbastefano, Dayse Pastore, Maria Clara Lippi. A novel predictive mathematical model for COVID-19 pandemic with quarantine, contagion dynamics, and environmentally mediated transmission. medRxiv 2020.07.27.20163063; doi: <https://doi.org/10.1101/2020.07.27.20163063>
12. Piotr T. Chruściel, Sebastian J. Szybka. Universal properties of the dynamics of the Covid-19 pandemics. medRxiv 2020.08.24.20181214; doi: <https://doi.org/10.1101/2020.08.24.20181214>
13. Gyan Bhanot, Charles DeLisi. Analysis of Covid-19 Data for Eight European Countries and the United Kingdom Using a Simplified SIR Model. medRxiv 2020.05.26.20114058; doi: <https://doi.org/10.1101/2020.05.26.20114058>
14. Lia Humphrey et al. TESTING, TRACING AND SOCIAL DISTANCING: ASSESSING OPTIONS FOR THE CONTROL OF COVID 19 . medRxiv 2020.04.23.20077503; doi: <https://doi.org/10.1101/2020.04.23.20077503>
15. Md. Haider Ali Biswas, M. S. Khatun, A. K. Paul, M. R. Khatun, M. A. Islam, S. A. Samad, U. Ghosh. Modeling the Effective Control Strategy for Transmission Dynamics of Global Pandemic COVID-19. medRxiv 2020.04.22.20076158; doi: <https://doi.org/10.1101/2020.04.22.20076158>
16. Elinor Aviv-Sharon, Asaph Aharoni. Forecasting COVID-19 pandemic Severity in Asia. medRxiv. doi: <https://doi.org/10.1101/2020.05.15.20102640>
17. Ashok Krishnamurthy. Spatiotemporal Transmission Dynamics of COVID-19 in Spain. Conference: Advancing knowledge about spatial modeling, infectious diseases, environment and health (June 8-12, 2020). Presentation.

- https://www.researchgate.net/publication/342247591_Spatiotemporal_Transmission_Dynamics_of_COVID-19_in_Spain
18. Nesteruk I. *COVID19 pandemic dynamics*. Springer Nature, 2021, <https://link.springer.com/book/10.1007/978-981-33-6416-5>
 19. Nesteruk I. Comparison of the First Waves of the COVID-19 Pandemic in Different Countries and Regions. In book: *COVID19 pandemic dynamics*. Springer Nature, 2021, https://link.springer.com/chapter/10.1007/978-981-33-6416-5_7
 20. <https://index.minfin.com.ua/reference/coronavirus/ukraine/>
 21. https://uk.wikipedia.org/wiki/%D0%A1%D0%BF%D0%B8%D1%81%D0%BE%D0%BA_%D0%BE%D0%B1%D0%BB%D0%B0%D1%81%D1%82%D0%B5%D0%B9_%D0%A3%D0%BA%D1%80%D0%B0%D1%97%D0%BD%D0%B8_%D0%B7%D0%B0_%D1%87%D0%B8%D1%81%D0%B5%D0%BB%D1%8C%D0%BD%D1%96%D1%81%D1%82%D1%8E_%D0%BD%D0%B0%D1%81%D0%B5%D0%BB%D0%B5%D0%BD%D0%BD%D1%8F
 22. https://en.wikipedia.org/wiki/List_of_European_countries_by_population
 23. https://en.wikipedia.org/wiki/European_countries_by_percentage_of_urban_population
 24. <https://www.indexmundi.com/map/?v=21000&r=eu&l=en>
 25. Draper NR, Smith H. Applied regression analysis. 3rd ed. John Wiley; 1998.
 26. <https://onlinepubs.trb.org/onlinepubs/nchrp/cd-22/manual/v2appendixc.pdf>
 27. Gazzola M., Argentina M. & L. Mahadevan. Scaling macroscopic aquatic locomotion. Nature Physics volume 10, pages 758–761 (2014).
 28. I. Nesteruk, “Maximal speed of underwater locomotion”, Innov Biosyst Bioeng, 2019, vol. 3, no. 3, pp. 152–167. Doi: <https://doi.org/10.20535/ibb.2019.3.3.177976>
 29. Nesteruk I. Visible and real sizes of new COVID-19 pandemic waves in Ukraine Innov Biosyst Bioeng, 2021, vol. 5, no. 2, pp. 85–96. DOI: 10.20535/ibb.2021.5.2.230487 <http://ibb.kpi.ua/article/view/230487>
 30. <https://podillyanews.com/2020/12/17/u-shkolah-hmelnytskogo-provely-eksperyment-z-testuvannyama-covid-19/>
 31. <https://edition.cnn.com/2020/11/02/europe/slovakia-mass-coronavirus-test-intl/index.html>
 32. <https://www.voanews.com/covid-19-pandemic/slovakias-second-round-coronavirus-tests-draws-large-crowds>
 33. Nesteruk I. Impact of vaccination and undetected cases on the COVID-19 pandemic dynamics in Qatar in 2021. [Preprint] MedRxiv, June 2021. DOI: [10.1101/2021.05.27.21257929](https://doi.org/10.1101/2021.05.27.21257929) <https://medrxiv.org/cgi/content/short/2021.05.27.21257929v1>
 34. Nesteruk I. The real COVID-19 pandemic dynamics in Qatar in 2021: SIR simulations, predictions and verifications. [Preprint] Research Gate, June 2021. DOI: [10.13140/RG.2.2.32904.55044](https://doi.org/10.13140/RG.2.2.32904.55044)
 35. <https://www.nytimes.com/2021/06/24/science/ancient-coronavirus-epidemic.html>